Influence of sickle hemoglobin polymerization and membrane properties on deformability of sickle erythrocytes in the microcirculation

Cheng Dong, Richard S. Chadwick, and Alan N. Schechter*

Biomedical Engineering and Instrumentation Program, National Center for Research Resources, and *Laboratory of Chemical Biology, National Institute of Diabetes and Digestive and Kidney Diseases, National Institutes of Health, Bethesda, Maryland 20892 USA

ABSTRACT The rheological properties of normal erythrocytes appear to be largely determined by those of the red cell membrane. In sickle cell disease, the intracellular polymerization of sickle hemoglobin upon deoxygenation leads to a marked increase in intracellular viscosity and elastic stiffness as well as having indirect effects on the cell membrane. To estimate the components of abnormal cell rheology due to the polymerization process and that due to the membrane abnormalities, we have developed a simple mathematical model of whole cell deformability in narrow vessels. This model uses hydrodynamic lubrication theory to describe the pulsatile flow in the gap between a cell and the vessel wall. The interior of the cell is modeled as a Voigt viscoelastic solid with parameters for the viscous and elastic moduli, while the membrane is assigned an elastic shear modulus. In response to an oscillatory fluid shear stress, the cell—modeled as a cylinder of constant volume and surface area—undergoes a conical deformation which may be calculated. We use published values of normal and sickle cell membrane elastic modulus and of sickle hemoglobin viscous and elastic moduli as a function of oxygen saturation, to estimate normalized tip displacement, d/h_o, and relative hydrodynamic resistance, R_r, as a function of polymer fraction of hemoglobin for sickle erythrocytes. These results show the transition from membrane to internal polymer dominance of deformability as oxygen saturation is lowered. More detailed experimental data, including those at other oscillatory frequencies and for cells with higher concentrations of hemoglobin S, are needed to apply fully this approach to understanding the deformability of sickle erythrocytes in the microcirculation. The model should be useful for reconciling the vast and disparate sets of data available on the abnormal properties of sickle cell hemoglobin and sickle erythrocyte membranes, the two main factors that lead to pathology in patients with this disease.

INTRODUCTION

The deformability properties of erythrocytes are critical determinants of flow in the microcirculation (Skalak, 1969; Evans and Hochmuth, 1976; Chien et al., 1982, 1987; Linderkamp and Meiselman, 1982; Nash and Meiselman, 1982; Nash et al., 1984, 1986; Pfafferott et al., 1985; Shohet and Mohandas, 1988). Abnormalities of these properties are thought to be the principal cause of the pathophysiology of sickle cell disease and other hemoglobinopathies (Schechter et al., 1987). Erythrocytes have evolved a complex membrane architecture, with a subskeletal network of proteins as well as a lipid bilayer with inserted proteins, which allows them to undergo extraordinary shape change as they traverse small vessels, such as terminal arterioles, precapillary sphincters, or the splenic sinuses (Shohet and Mohandas, 1988).

In diseases of hemoglobin, such as the thalassemia syndromes, the unstable hemoglobin diseases, and especially sickle cell disease, this crucial deformability is altered, leading to hemolysis and anemia as well as tissue damage. In the sickle syndromes these abnormal rheological properties are believed to be caused primarily by the increase in internal red cell viscosity due to the aggregation or polymerization of sickle hemoglobin (Hb S) upon deoxygenation, as well as biochemical abnormalities in the membrane of the sickle erythrocyte. These membrane changes, both reversible and irreversible, are thought to occur due to repeated cycles of polymerization–depolymerization during the life of the sickle erythrocyte in the bone marrow and circulation (Hebbel, 1991). Other rheological abnormalities may occur because of the shrinkage of certain sickle cells (the dense cells) so that they have a very high mean corpuscular hemoglobin concentration (MCHC) (>40 g/dl) which elevates internal viscosity, even of the oxygenated Hb S. Irreversible membrane abnormalities due to precipitated hemoglobin chains or heme groups or to reversible interaction of the Hb S with the red cell membrane cytoskeleton may also occur in the hemoglobinopathies.

In recent years the polymerization of Hb S inside sickle erythrocytes has been well characterized (Noguchi and Schechter, 1985; Schechter et al., 1987; Eaton and Hofrichter, 1987, 1990) as a function of physiologically relevant variables, such as MCHC, pH, and oxygen saturation. Extensive clinical studies of the effects of the abnormal sickle erythrocytes in patients have been reported (Rodgers et al., 1984; Francis and Johnson, 1991). A central remaining goal in sickle cell rheology is to ascertain the relative importance of the internal Hb S and the sickle cell membrane to the overall properties of sickle cells in the microcirculation.

EXPERIMENTAL AND THEORETICAL BACKGROUND

Many methods to measure red cell deformability have been used (Klug et al., 1974; Chien, 1977; Mohandas et al., 1979). The methods most commonly used to study erythrocyte suspensions are viscometry (Dintenfass, 1964; Charache and Conley, 1964; Chien et al., 1970,

0006-3495/92/08/774/10 $2.00

1982; Drasler et al., 1989), filtration (Weed et al., 1969; Messer and Harris, 1970; Chien et al., 1971; Lessin et al., 1977; Reinhart et al., 1984; Arai et al., 1990), and ektacytometry (Bessis and Mohandas, 1975, 1977; Groner et al., 1980; Sorette et al., 1987). The micropipette technique is useful to study single cell deformability, including cell membrane properties (Evans and Hochmuth, 1976; LaCelle et al., 1977; Nash et al., 1984). In addition to cell suspension studies, viscometry is also useful for determining the rheological properties of Hb S solutions (Briehl, 1981; Chien et al., 1982; Danish et al., 1987; Drasler et al., 1989). Recent experimental studies have shown that the overall rheological properties of sickle erythrocytes are strongly influenced by both cell membrane viscoelasticity (Nash et al., 1984; Evans et al., 1984; Drasler et al., 1989; Messmann et al., 1990; Hebbel, 1991) and interior Hb S gelation (Briehl, 1981; Hofrichter et al., 1981; Gabriel et al., 1981; Noguchi and Schechter, 1985; Eaton and Hofrichter, 1987, 1990; Danish et al., 1987, 1989; Clark, 1989).

The purpose of this investigation is to develop a simple mathematical formulation of the rheological properties of the erythrocytes in the microcirculation and to apply such a model to the special behavior of the sickle erythrocyte. A corollary of this is to ascertain the relative contributions of the red cell membrane and the internal Hb S solution to the viscous and elastic components of total cell deformability during passage through the circulation, particularly at different oxygen saturation levels. Alternatively, these relative contributions can also be expressed as a function of polymer fraction via the data shown in Fig. 1 *a*. The data published by Chien et al. (1982), while not complete, are a useful starting point to elucidate the roles of these individual components of the sickle erythrocytes in determining their behavior in microcirculation with respect to the parameters of the model.

An unsteady shear applied to the cell body is needed to assess both the viscous and elastic components of interior Hb S gelation. Chien et al. (1982) performed such experiments to measure both viscous and elastic components of complex viscosity (denoted by η' and η'') in a Hb S solution at a concentration of 32 g/dl under shear oscillating at low frequency (Fig. 1, *b* and *c*). The tests were made in a Weissenberg rheogoniometer that had been modified to provide a cone-and-plate geometry. That study illustrated that the viscous (η') and elastic (η'') components began to increase when the oxygen saturation of the solution was reduced to ~80%. It was stated in their study that the elevation of both η' and η'' with reductions in oxygen saturation was most pronounced at low frequencies of oscillation (0.015 Hz). According to these data, the critical level of oxygen saturation at which a large increase in magnitude of η' and η'' becomes appar-

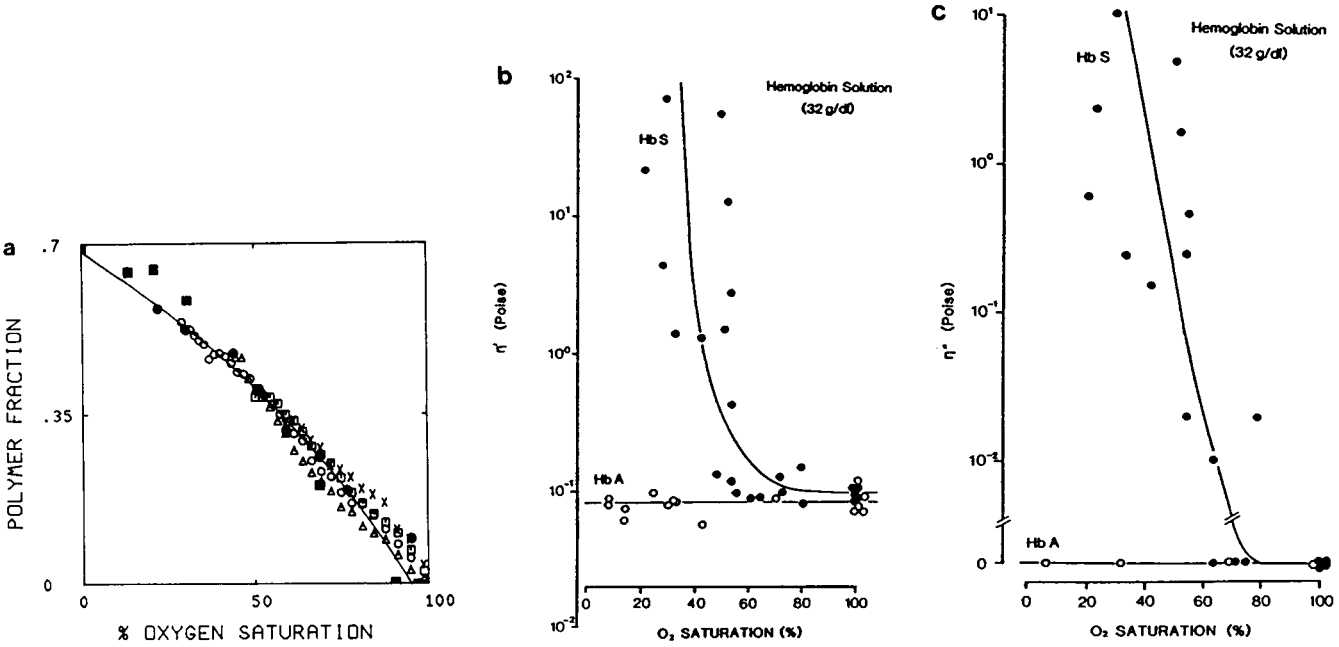

FIGURE 1 (*a*) ^{13}C NMR measurements of the fraction of polymerized hemoglobin in SS erythrocytes as a function of oxygen saturation. (Reproduced from *Proc. Natl. Acad. Sci. USA.*, 1980, 77:5487–5491, by permission.) Data from different patients are indicated by different symbols. (*b*) The viscous component of complex viscosity (η') of Hb S and Hb A solutions (concentrations at 32 g/dl) as a function of O_2 saturation. Data were obtained at a frequency of 0.015 Hz. (*c*) The elastic component of complex viscosity (η'') of Hb S and Hb A solutions (concentration at 32 g/dl) as function of O_2 saturation. Data were obtained at frequency of 0.015 Hz. (Panels *b* and *c* reproduced from *Blood Cells (NY)*, 1982, 8:53–64, by permission.)

ent is strongly dependent on the Hb S solution concentration as well as the oscillatory frequency. However, their experimental results are only available under low frequency with Hb S concentration at 32 g/dl, which is equivalent to the concentration of hemoglobin in the mean density sickle red cell, not the dense cells that are so characteristic of the disease. Drasler et al. (1989) reported studies on the frequency-dependent viscoelasticity of oxygenated sickle cell suspensions as well as Hb S solutions in an oscillating viscometer, but no data are available as a function of oxygen saturation level. Nevertheless, the results from either Chien et al. (1982) or Drasler et al. (1989) suggest that the presence of both the cell membrane and the internal Hb S is a major factor in determining the viscoelastic behavior of sickle cells during deoxygenation.

Previous mathematical descriptions of normal red blood cell in capillaries have treated the cell interior as Newtonian fluid. The shape of the cell is assumed to be steady so the fluid within the cell produces only a constant pressure field (e.g., Secomb et al., 1986). This assumption for the cell interior will not be valid for the sickle cell hemoglobin due to Hb S polymerization. In the study of sickle cell capillary flow, Berger and King (1980) treated the oxyrheology as a cell membrane phenomenon by using the Krogh model for oxygen transport between sickle cell blood (or capillary) and tissue regions. Other studies of Hb S gelation, however, have shown extensive polymer in the cytoplasm of deoxygenated cells. Thus a more accurate model should account for both contributions from the cell membrane and hemoglobin in sickle cell rheology.

MATHEMATICAL FORMULATION AND SOLUTION METHOD

The deformation and flow of erythrocytes through narrow cylindrical vessels is modeled mathematically as shown in Fig. 2. The unstressed geometry of each cell is approximated by a circular cylinder consisting of a viscoelastic interior bounded by an elastic membrane. This cylinder is constrained to have a volume (92 μ^3) and surface area (130 μ^2) similar to that of an erythrocyte. Thus the reference length (L) is 2.4 μm and the reference radius (a) is 3.5 μm. The volume and surface area remain constant throughout the induced deformation. The capillary is taken as a rigid circular tube of radius R_0. The analytical results are limited to cases in which one cell occupies a given section of the tube at a given time and the vessel radius is larger than the cell reference radius. Lubrication theory is used to describe the pulsatile flow of the suspending fluid in the gap denoted by h_0 between a cell and the vessel wall. This suspending fluid (plasma phase) is assumed to be an incompressible Newtonian fluid with a viscosity μ_p of 1.2 centipoise (Cokelet, 1972). The model takes into account the elastic properties of the red blood cell membrane, especially its response to shear. The cell interior is assumed to be a Voigt viscoelastic solid to represent the properties of Hb S solution for which the model parameters μ_s (dyn · sec/cm^2) and E_s (dyn/cm^2) are viscous and elastic moduli, respectively. During Hb S gelation, these parameters are considered as a function of a total amount of polymer formed inside sickle cells or as a function of oxygen saturation at a given Hb S concentration.

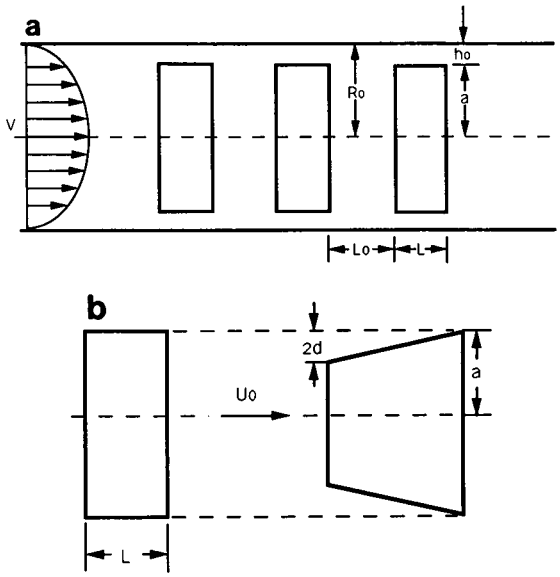

FIGURE 2 (a) Model of red blood cells in capillary. a is the cell radius; L is the cell length; h_0 is the gap between the cell and capillary wall; L_0 is the distance between cells; V is the velocity of suspending plasma; and R_0 is the vessel radius. (b) Model of red blood cell shapes in resting and deformed states. $2d$ is the deflection of the trailing edge and U_0 is the cell velocity.

An incompressible viscoelastic continuum is adopted for the cell interior. It is convenient to introduce complex-valued field variables to deal with the pulsatile nature of the flow. Let $\vec{U}^*$ be a complex displacement vector that satisfies quasi-static equilibrium as follows:

$$0 = -\nabla P^* + \mu^* \nabla^2 \vec{U}^*, \tag{1}$$

where P^* is a complex hydrostatic pressure and μ^* is the complex shear modulus of the interior viscoelastic material. For Voigt viscoelastic solid, μ^* can be expressed in terms of its elastic (E_s) and viscous (μ_s) components by:

$$\mu^* = E_s + i2\pi f \mu_s, \tag{2}$$

where f is the oscillation frequency. The continuity equation for an incompressible Voigt solid can be written as:

$$\nabla \cdot \vec{U}^* = 0. \tag{3}$$

In terms of cylindrical coordinates (r, z, θ), a general solution for Eqs. 1 and 3 is given by Happel and Brenner

(1965). In the case of axisymmetry as assumed here (no dependence on θ), the solution can be represented by:

$$U_r^* = \frac{\partial \psi^*}{\partial r} + r\frac{\partial^2 \Pi^*}{\partial r^2}$$

$$U_z^* = \frac{\partial \psi^*}{\partial z} + r\frac{\partial^2 \Pi^*}{\partial r \partial z} + \frac{\partial \Pi^*}{\partial z}$$

$$P^* = -2\mu^* \frac{\partial^2 \Pi^*}{\partial z^2}, \tag{4}$$

where U_r^* and U_z^* are, respectively, the complex-valued displacement components of the cell interior in radial and axial directions, and ψ^* and Π^* are arbitrary complex-valued harmonic functions. For convenience of the analytical approach, it is further assumed that two ends of the cylinder remain flat, i.e., $\partial U_z^*/\partial r = 0$ at $z = 0, L$. In other words, the cell interior is considered to be bounded by two circular rigid plates at the ends that can deform freely in their planes, and a cylindrical membrane on the lateral surface. Thus we take:

$$\psi^* = \sum_{n=1}^{\infty} B_n^* I_0(\beta_n r)\cos(\beta_n z)$$

$$\Pi^* = C_0^*\left[r^2 - 2\left(z - \frac{L}{2}\right)^2\right] + \sum_{n=1}^{\infty} \frac{C_n^*}{2\mu^*\beta_n^2} I_0(\beta_n r)\cos(\beta_n z), \tag{5}$$

in which I_0 is the 0th order modified Bessel function in first kind; B_n^*, C_0^*, and C_n^* are arbitrary constants that must be determined, and $\beta_n = n\pi/L$, $n = 1, 2, \ldots$.

For the exterior layer, membrane theory is applied to the lateral surface of the cylinder by neglecting bending energy and changes in membrane thickness. It is assumed that the membrane surface area is conserved locally, which implies the existence of the isotropic tension T_0^* (a complex-valued stress resultant, in dyn/cm). Let u_r^* and u_z^* be the complex-valued membrane displacement components defined in the cylindrical coordinates (r, z, θ) at $r = a$, and T_θ^* and T_z^* be the complex-valued membrane tensions in the circumferential and axial directions due to the elastic shear on the surface. Then the constitutive equations of the membrane can be written as:

$$T_\theta^* = T_0^* + 2\mu_m \frac{u_r^*}{a}$$

$$T_z^* = T_0^* + 2\mu_m \frac{\partial u_z^*}{\partial_z}, \tag{6}$$

where μ_m is the membrane elastic shear modulus (in dyn/cm). The equations of membrane equilibrium are given by:

$$\frac{T_\theta^*}{a} = -\sigma_{rr|_{r=a}}^* - p_f^*$$

$$\frac{\partial T_z^*}{\partial z} = \tau_w^* + \sigma_{rz|_{r=a}}^*. \tag{7}$$

$\sigma_{rr|_{r=a}}^*$ and $\sigma_{rz|_{r=a}}^*$ are the complex-valued loads applied by the interior viscoelastic material in radial and axial directions, respectively, which can be obtained from the constitutive relations and evaluated at the surface $r = a$:

$$\sigma_{rr}^* = -P^* + 2\mu^* \frac{\partial U_r^*}{\partial r}$$

$$\sigma_{rz}^* = \mu^*\left(\frac{\partial U_r^*}{\partial z} + \frac{\partial U_z^*}{\partial r}\right). \tag{8}$$

The displacement components are continuous on the lateral boundary at $r = a$; i.e., $u_r^*(z) = U_r^*(a, z)$ and $u_z^*(z) = U_z^*(a, z)$.

The complex-valued loads on the membrane surface due to the suspending fluid, p_f^* and τ_w^*, are also included in the membrane equations (Eq. 7). We estimated these loads using hydrodynamic lubrication theory. We first determined the cylinder deformations based on fluid loading in a gap of constant thickness, $h_0 = R_0 - a$. The resulting deformations are then used to determine a variable gap $h = h(z)$ and the resulting hydrodynamic resistance. The complex-valued fluid shear stress τ_w^* acting on the lateral surface of the undeformed cell is given approximately by:

$$\tau_w^* \cong \mu_p \frac{V_m^*}{h_0} \tag{9}$$

where

$$V_m^* = \overline{V_m} + V_0 e^{i2\pi ft}. \tag{10}$$

Here $\overline{V_m}$ is the given temporal average of the spatial mean flow velocity upstream of the cell, V_0 is the given oscillation amplitude, f is the frequency, and t is time. Eq. 9 requires some further explanation because of its approximate nature. As written, it represents the fluid shear stress produced on a flat surface translating axially with velocity $\overline{V_m}$ at a distance h_0 from a stationary surface. This is a good approximation since: (a) the Womersley parameter, $h_0(2\pi f\rho/\mu_p)^{1/2} \ll 1$ (ρ is the plasma density); and (b) the dimensionless gap h_0/a is small. This latter condition (b) allows us to neglect the effect of wall curvature and also implies that the cell translates with axial velocity $\overline{V_m}[1 + O(h_0/a)]$ (Tözeren and Skalak, 1978). The pressure distribution in the gap, $p_f^*(z)$, can be determined as follows. The pressure drop across the cell can be determined by requiring that the net force due to the pressure drop acting on the ends of the cylinder must balance the net force due to the fluid shear acting on the lateral side of the cylinder; i.e.,

$$\pi a^2 \Delta p_f^* = 2\pi a L \tau_w^*. \tag{11}$$

Since this pressure drop occurs over the length L of the cell, and the pressure must be a decreasing linear function of z when the gap is constant, we have

$$p_f^*(z) = 2(L/a)\tau_w^*(L - z). \tag{12}$$

The unknown constants C_n^* can be related to the B_n^* by requiring that the lateral surface maintains locally constant area during deformation; i.e.,

$$\frac{\partial u_z^*}{\partial z} + \frac{u_r^*}{a} = 0 \tag{13}$$

on $r = a$. The constants C_0^* and B_n^* can then be determined by expanding the loads in a Fourier series over the interval $0 < z < L$, and using Eqs. 4–8 together with the conditions of continuity of displacements and tractions at the interface of the interior viscoelastic cylinder and the exterior cylindrical membrane at $r = a$. The physical cell deformation can be obtained by taking the real part of the complex-valued solution if the spatial mean flow velocity upstream of the cell (cf. Eq. 10) is assumed to be $V_m = \overline{V_m} + V_0 \cos(2\pi f t)$.

CELL DEFORMATION AND HYDRODYNAMIC RESISTANCE INDICES

The deformed cylinder has a shape that can be approximated by a frustum of a cone that is narrowest at the trailing edge, as shown in Fig. 2 *b*. The half-deflection of the trailing edge, denoted by d, serves as a deformation index. This shape reflects the effects of the hydrodynamic loading conditions in the gap. The negative radial deformation is greatest at the trailing edge where the gap pressure is greatest (cf. Eq. 12). The mean gap pressure, $p_m^* = (L/a)\,\tau_w^*$, which determines the constant C_0^*, has the effect of uniformly compressing and elongating the cylinder, while the gap pressure gradient slants the lateral surface. The uniform compression mode, while maintaining constant cell volume, requires fine-scale wrinkling of the membrane in order to maintain constant membrane surface area. For this mode only, membrane wrinkling requires that Eq. 13 be replaced with the condition of vanishing isotropic tension T_0^*.

The relative resistance ratio, R_r, is the ratio of the pressure drop across the deformable cell, Δp_{def}, to that of the rigid cell, Δp_{rig}. The later is given by Eqs. 9 and 11. To calculate the former we can use lubrication theory with a variable gap $h = h(z)$ (Batchelor, 1967). We introduce a new variable, x, defined by $r = R_0 - h(z) + x$, which measures the radial distance from the cell lateral surface ($x = 0$) to the tube wall ($x = h(z)$). The essential approximation of lubrication theory is that axial velocity profile, $V_z(x, z)$, is a quadratic function of x; i.e.,

$$V_z(x, z) = U_0\left(1 - \frac{x}{h}\right) + \frac{1}{2\mu_p}\frac{dp_f}{dz}[x(x - h)]. \tag{14}$$

The coefficients of x have been chosen such that V_z vanishes on $x = h$ (no-slip condition) and $V_z = U_0$, the unknown cell velocity, on $x = 0$. In addition to Eq. 14, two conservation laws are required to determine Δp_{def}. The first is conservation of volume flux. Consider two planes spanning the vessel and perpendicular to its axis, one upstream of the cylinder and the other cutting through it. The volume flux crossing these planes must be identical since both the fluid and the cell are incompressible. Therefore,

$$\pi R_0^2 V_m = \pi(R_0 - h)^2 U_0 + 2\pi \int_0^h (R_0 - h + x) V_z(x, z)\, dx, \tag{15}$$

where $V_m = \overline{V_m} + V_0$ (cf. Eq. 10). Substitution of Eq. 14 into Eq. 15 and performing the integration yields:

$$\frac{dp_f}{dz} = \frac{12\mu_p[U_0(R_0^2 - R_0 h + h^2/3)] - R_0^2 V_m]}{h^3(2R_0 - h)}. \tag{16}$$

Taking $h(z) = h_0 + 2d(1 - z/L)$, which approximates the variable gap shape with the deformed cell, and integrating Eq. 16 over $0 \le z \le L$ yields an expression for the pressure drop, Δp_{def}, across the deformed cell. However, since that expression involves the unknown cell velocity, U_0, we need to invoke another conservation law. Consider the control volume bounded by the deformed cell surface, the tube wall, and two planes perpendicular to the tube axis, one just upstream of the cell and the other just downstream. Tözeren and Skalak (1978) pointed out that because of the zero drag condition the cell contributes zero net axial force on the control volume. Therefore the axial force from the pressure drop across the cell is exactly balanced by the integral of the fluid shear stress acting on the *tube* wall; i.e.,

$$\pi R_0^2 \Delta p_{def} = -2\pi R_0 \mu_p \int_0^L \frac{\partial V_z(h, z)}{\partial x}\, dz. \tag{17}$$

Substitution of Eqs. 14 and 16 into Eq. 17 and performing the integration yields another equation for Δp_{def} involving the unknown particle velocity U_0. These two equations constitute a linear algebraic system for the determination of Δp_{def} and U_0.

COMPUTED RESULTS

Hb S rheology

An alternative way to present the experimental data published by Chien et al. (1982) is shown in Fig. 3, *a* and *b*, where it is plotted in terms of the elastic (E_s) and viscous (μ_s) components of the complex shear modulus (cf. Eq. 2) as a function of oxygen saturation. Both elastic and viscous components in the Hb S solution increase when the oxygen saturation decreases. The rheological properties of the Hb S solution during oxygenation or deoxygenation can be seen through the change of a phase angle β that is calculated from the complex shear modulus

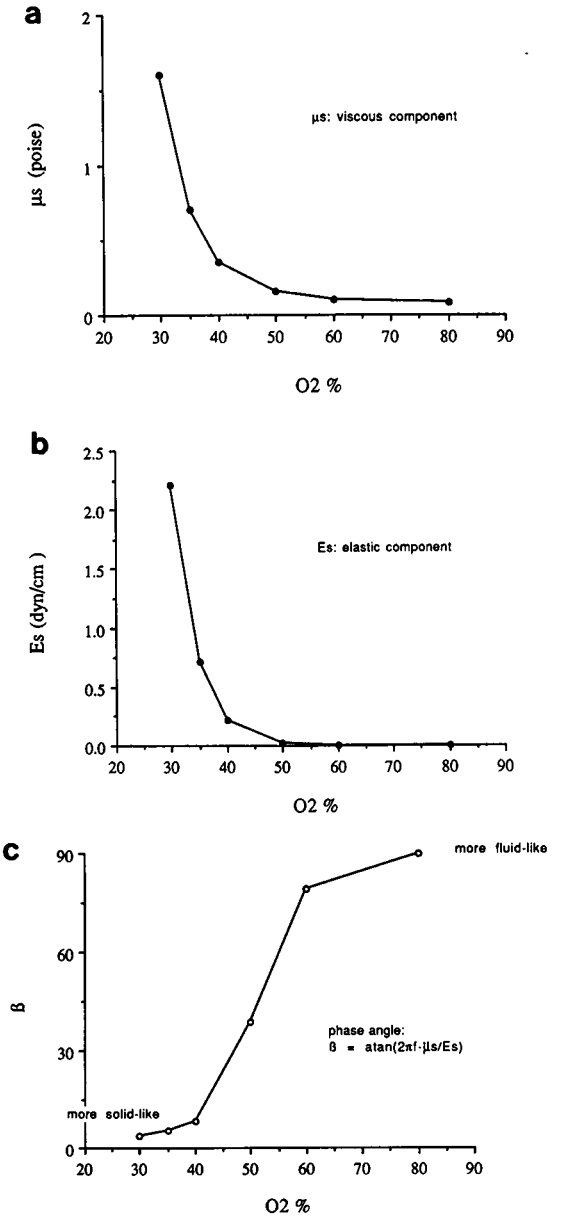

FIGURE 3 (*a* and *b*) An alternative representation of the data shown in Fig. 1, *b* and *c*; E_s and μ_s are the elastic and viscous components, respectively. (*c*) The phase angle (β) calculated from the complex shear modulus. f is the oscillation frequency.

(Fig. 3 *c*). This phase angle is a function of both the oxygen saturation and the oscillation frequency. Fig. 3 illustrates that despite qualitatively similar changes in E_s and μ_s, the Hb S solution behaves in a more fluid-like manner when it is oxygenated (so called "out-of-phase" behavior, when the phase angle of the complex shear modulus approaches 90°), whereas it behaves in a more solid-like manner when it is deoxygenated (so called "in-phase" behavior, when β approaches 0°), as expected of the Hb S polymer.

Cell deformation index

Fig. 4 *a* shows the computed normalized trailing edge half-displacement d/h_0 as the function of polymer fraction for various values of the cell membrane elasticity μ_m. This index is evaluated at the time during the cycle when d is maximal. It can be seen that the cell becomes less deformable when polymer fraction rises above 0.4–0.45 (μ_m = 0.01 dyn/cm is the expected value for the normal erythrocyte; Evans and Hochmuth, 1976). Increasing the membrane elastic modulus (μ_m), as may be expected to occur in sickle erythrocytes (Nash et al., 1986), decreases the cell deformability within the physiological range of oxygen saturation. However, membrane elasticity will have less effect for a very high polymer fraction (the curve with open circles will meet the other

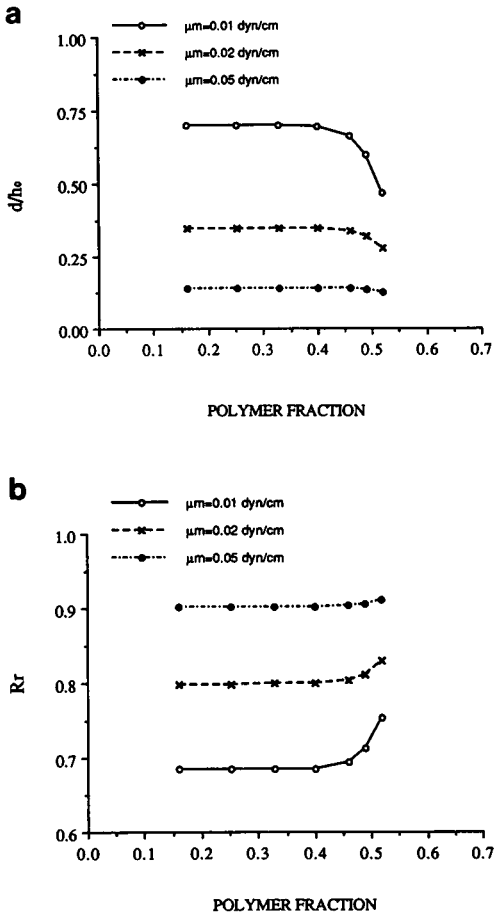

FIGURE 4 (*a*) The calculated normalized tip half displacement (d/h_0) of a cell as a function of polymer fraction. (*b*) The calculated ratio of the flow resistance (Rr) of deformable cells to that of rigid cells at different polymer fraction. The results in *a* and *b* are computed with selected membrane elastic shear modulus (μ_m): μ_m = 0.01, 0.02, and 0.05 dyn/cm; cell radius a = 3.5 μ; cell length L = 2.4 μm; gap h_0 = 0.4 μm; mean velocity $\overline{V_m}$ = 0.1 cm/s; velocity oscillatory amplitude = 0.01 cm/s; oscillatory frequency f = 0.015 Hz; plasma viscosity μ_p = 0.012 poise; hemoglobin concentration Ct = 32 g/dl.

two at a high polymer fraction level, where changing μ_m does not change d/h_0 significantly). This shows that the rheological influence from the interior Hb S solution will exceed that from the membrane and therefore dominate the overall cell deformability at high polymer fraction levels. Due to the only available data shown in Fig. 1, *b* and *c*, the graph does not go beyond the point of polymer fraction > 0.52 (i.e., when O_2 saturation is <30%).

Hydrodynamic resistance

The resistance index, R_r, calculated at the time when d is maximal, is plotted in Fig. 4 *b* as a function of polymer fraction for various values of the cell membrane elasticity μ_m. R_r increases when the membrane elastic modulus or polymer fraction increases. The critical change happens at a polymer fraction level of 0.4–0.45. It can also be seen that the critical level of polymer fraction increases slightly when membrane elasticity μ_m increases. However, when polymer fraction is >0.52, the cell membrane starts to lose its mechanical importance and the Hb S solution controls the hydrodynamic resistance.

DISCUSSION

A simple model of the influence of the internal Hb S solution and the properties of the membrane as a function of oxygen saturation on the deformability and thus the hydrodynamic resistance of sickle erythrocytes in narrow vessels is presented. The model uses previously published experimental data to explain how the amount of polymer inside a sickle cell might affect the total cell rheological behavior through an approximate theory and the use of one set of relevant data.

The model indicates that cells become less and less deformable when the amount of polymer inside a sickle cell rises above 0.4–0.45 in volume fraction (or when oxygen saturation drops below 40–50% [Fig. 1 *a*]), if the membrane rigidity has a value representative of a normal cell (μ_m = 0.01 dyn/cm). The flow resistance of the cells increases significantly when oxygen saturation decreases to this critical level. Change of membrane rigidity can also affect the intrinsic cell deformability and flow resistance (e.g., increasing μ_m from 0.01 dyn/cm to larger values, as shown in Fig. 4 *a*) as well as the shape of the curves in Fig. 4, *a* and *b*. Cell membrane elasticity certainly becomes the major determinant of overall cell deformability when the Hb S solution is fully oxygenated. Fig. 4 *a* suggests that the rheological importance of the internal Hb S can exceed that from the membrane when the polymer fraction is >0.52 (where all curves intersect independent of the value of μ_m). This conclusion was also reached by Chien et al. (1982) by comparing viscosity data from Hb S solutions and sickle cell suspensions at varying O_2 saturations. (Their suggestion

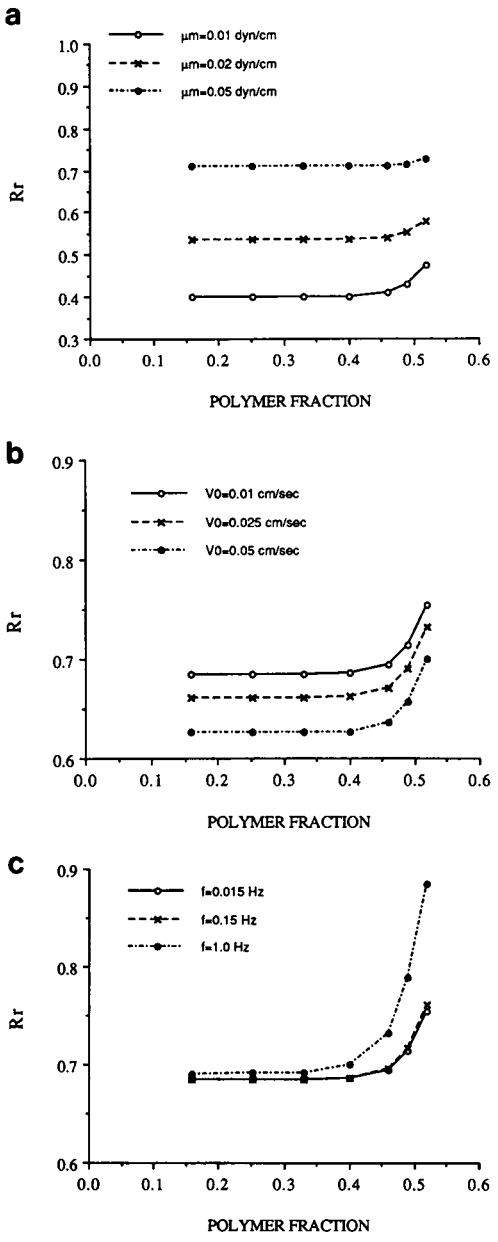

FIGURE 5 (*a*) Gap thickness effect on the flow resistance index (Rr). Same parameter values as in Fig. 4 except h_0 = 0.2 μm. (*b*) Oscillatory velocity amplitude (V_0) effect on the flow resistance index (Rr). Same parameter values as in Fig. 4. (*c*) Oscillatory frequency parameter (f) effect on the flow resistance index (Rr). Same parameter values as in Fig. 4.

that a theoretical analysis based on their data would be beneficial in further elucidating the relative roles of the cell membrane and internal hemoglobin to cell deformability in the microcirculation was a primary impetus for the present study.) The effects of changing the gap thickness and the amplitude of the flow oscillation on the resistance index are shown separately in Fig. 5, *a* and *b*. Decreasing the gap and increasing the flow oscillation amplitude both have the effect of decreasing the resis-

tance index without changing the critical value of polymer fraction.

Several factors can contribute to altering the critical value of polymer fraction. First, the sensitivity of cell deformation and hydrodynamic resistance indices to scatter in the data of Chien et al. (1982) can be investigated by constructing smooth curves that bound the data sets of Fig. 1, *b* and *c*. We have recalculated the curves for Fig. 3, *a* and *b* for data that (*a*) lie inside the band, (*b*) bound the data on the right, and (*c*) bound the data on the left, for the case $\mu_s = 0.01$ dyn/cm. These plots (not shown) could cause a left-shift of the critical value of polymer fraction to values as low as ~0.33 from 0.52. Second, increasing the oscillatory frequency parameter tends to shift the resistance index to the left as seen in Fig. 5 *c*. Third, a membrane rigidity dependence on oxygen saturation can significantly alter the shape of the resistance vs. polymer fraction curves. With the membrane rigidity depending on oxygen saturation as shown in Fig. 6 *a*, which is suggested by the effective membrane rigidity data of Nash et al. (1986), the resistance index predicted by the model in Fig. 6 *b* shows a much greater sensitivity to oxygen saturation than cells having a constant membrane rigidity. In fact, the concept of a critical

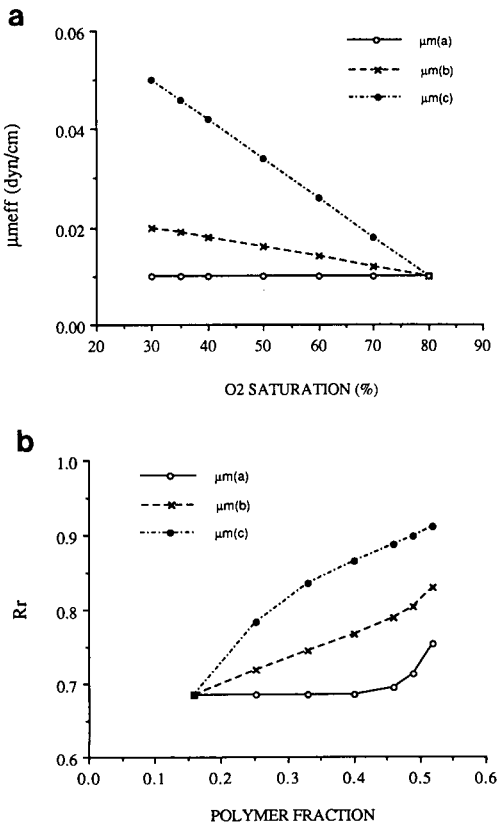

FIGURE 6 (*a*) Assumed dependence of membrane rigidity on oxygen saturation. (*b*) Effect of oxygen-dependent membrane rigidity on the flow resistance index (*Rr*). Otherwise, the same parameter values as in Fig. 4.

polymer fraction no longer applies. In other words, small amounts of polymer in this case can significantly affect whole cell deformability. The mechanism of membrane rigidity dependence on oxygen saturation is still unclear. A membrane–hemoglobin interaction is one possibility, as is the effect of ATP depletion even in normal cells (LaCelle, 1970). Such results would be consistent with the data of Green et al. (1988), which showed great sensitivity of sickle cell filtration to decreased oxygen saturation. The existence of a significant fraction of dense cells would also have this effect.

While this study is satisfying from the standpoint of using viscometry data in a relatively simple theoretical model to predict cell deformation and flow resistance in the microcirculation, many questions remain that suggest the need for both further experiments and a more sophisticated model. The viscometry data are incomplete with regards to the influence of both frequency and mean intracellular hemoglobin concentration. Values at the frequency close to that in the blood circulation (~1 Hz) will be important for better estimation of physiological properties. Although the present calculation is based on the low frequency data provided in Fig. 1, *b* and *c*, it still differs from the results obtained from a steady shear. Oscillations or other kinds of unsteady shear applied experimentally to the cell body are needed to assess both viscous and elastic components of interior Hb S gelation.

In addition to the need for further experiments, the model itself could be extended in several ways. It is known that the normal red blood cell membrane has a viscous behavior (Evans and Hochmuth, 1976), which implies a complex membrane shear modulus. The present analysis neglects this effect, and assumes that the viscous behavior is dominated by the cell interior. Clearly this is an important point that requires further study. Also, the computed cone shape is different from the classic parachute shape of deformed red blood cell in capillaries (Skalak, 1969; Secomb et al., 1986). The difference is due to the simplification that the deformed cylinder maintains flat ends, which enabled us to obtain an analytical solution with the viscoelastic interior. Also, the present model requires a reference hydrodynamic gap thickness to be specified, with the implication that the vessel diameter must be larger than the reference diameter of the cell.

The computed results illustrate the striking dependence of sickle cell deformability on the internal elasticity and viscosity of the intracellular Hb S solution during polymerization (as well as the membrane elasticity at high O_2 saturation) in our model, and predict the relative roles of the cell membrane and internal fluid to the overall rheology of the cell as a function of oxygen saturation. We hope that the model will provide a framework for analyzing the components of sickle cell rheology as data with other techniques and at other physiological variables become available.

The authors wish to thank Dr. Constance T. Noguchi and Dr. Griffin P. Rodgers (Laboratory of Chemical Biology, National Institute of Diabetes and Digestive and Kidney Disease, National Institutes of Health, Bethesda, MD) and Dr. Nobuhiro Uyesaka (Nippon Medical School, Tokyo, Japan) for many helpful discussions.

Received for publication 5 August 1991 and in final form 2 March 1992.

REFERENCES

Arai, K., M. Iino, and N. Uyesaka. 1990. Further investigations of red cell deformability with nickel mesh. *Biorheology.* 27:47–65.

Batchelor, G. K. 1967. An Introduction to Fluid Dynamics. Cambridge University Press, New York, 219–221.

Berger, S. A., and W. S. King. 1980. The flow of sickle-cell blood in the capillaries. *Biophys. J.* 29:119–148.

Bessis, M., and N. Mohandas. 1975. A diffractometric method for the measurement of cellular deformability. *Blood Cells (NY).* 1:307–313.

Bessis, M., and N. Mohandas. 1977. Laser diffraction patterns of sickle cells in fluid shear fields. *Blood Cells (NY).* 3:229–239.

Briehl, R. W. 1981. Rheological properties of the gelled phase of hemoglobin S. *In* The Molecular Basis of Mutant Hemoglobin Dysfunction. P. B. Sigler, editor. Elsevier North Holland, Inc., New York. 237–252.

Charache, S., and C. L. Conley. 1964. Rate of sickling of red cells during deoxygenation of blood from persons with various sickling disorders. *Blood.* 24:25–48.

Chien, S. 1977. Principles and techniques for assessing erythrocyte deformability. *Blood Cells (NY).* 3:71–99.

Chien, S., S. Usami, and J. F. Bertles. 1970. Abnormal rheology of oxygenated blood in sickle cell anemia. *J. Clin. Invest.* 49:623–634.

Chien, S., S. Luse, and C. Bryant. 1971. Hemolysis during filtration through micropores: a scanning electron microscopic and hemorrheologic correlation. *Microvasc. Res.* 3:183–203.

Chien, S., R. G. King, A. A. Kaperonis, and S. Usami. 1982. Viscoelastic properties of sickle cells and hemoglobin. *Blood Cells (NY).* 8:53–64.

Chien, S., A. A. Kaperonis, R. G. King, H. H. Lipowsky, E. A. Schmalzer, L. A. Sung, K. L. P. Sung, and S. Usami. 1987. Rheology of sickle cells and its role in microcirculatory dynamics. *In* Pathophysiological Aspects of Sickle Cell Vaso-occlusion. R. L. Nagel, editor. Alan R. Liss, Inc., New York. 151–165.

Clark, M. R. 1989. Mean corpuscular hemoglobin concentration and cell deformability. *Ann NY Acad. Sci.* 565:284–294.

Cokelet, G. R. 1972. The rheology of human blood. *In* Biomechanics: Its Foundations and Objectives. Y. C. Fung, N. Perrone, and M. Anliker, editors. Prentice-Hall, Inc., Englewood Cliffs, NJ. 63–103.

Danish, E. H., J. W. Harris, C. R. Moore, and I. M. Krieger. 1987. Rheologic behavior of deoxyhemoglobin S gels. *J. Mol. Biol.* 196:421–431.

Danish, E. H., J. W. Harris, and K. Oh. 1989. Solidity of sickle hemoglobin gels: relevance to pathophysiology of sickling disorders. *Clevel. Clin. J. Med.* 56:793–800.

Dintenfass, L. 1964. Rheology of packed red blood cells containing hemoglobins A-A, S-A, and S-S. *J. Lab. Clin. Med.* 64:594–600.

Drasler, W. J., M. S. Clark, and H. K. Keller. 1989. Viscoelastic properties of the oxygenated sickle erythrocyte membrane. *Biorheology.* 26:935–949.

Eaton, W. A., and J. Hofrichter. 1987. Hemoglobin S gelation and sickle cell disease. *Blood.* 70:1245–1266.

Eaton, W. A., and J. Hofrichter. 1990. Sickle cell hemoglobin polymerization. *Adv. Protein Chem.* 40:63–279.

Evans, E. A., and R. M. Hochmuth. 1976. Membrane visco-elasticity. *Biophys. J.* 16:1–12.

Evans, E. A., N. Mohandas, and A. Leung. 1984. Static and dynamic rigidities of normal and sickle erythrocytes. *J. Clin. Invest.* 73:477–488.

Francis, R. B., and C. S. Johnson. 1991. Vascular occlusion in sickle cell disease. Current concepts and unanswered questions. *Blood.* 77:1405–1414.

Gabriel, D. A., L. A. Smith, and C. S. Johnson. 1981. Elastic properties of deoxy hemoglobin S (Deoxy-HBS) gel. *Arch. Biochem. Biophys.* 211:774–776.

Green, M. A., C. T. Noguchi, A. J. Keidan, S. S. Marwah, and J. Stuart. 1988. Polymerization of sickle cell hemoglobin at arterial oxygen saturation impairs erythrocyte deformability. *J. Clin. Invest.* 81:1669–1674.

Groner, W., N. Mohandas, and M. Bessis. 1980. New optical technique for measuring erythrocyte deformability with the ektacytometer. *Clin. Chem.* 26:1435–1442.

Happel, J., and H. Brenner. 1965. Low Reynolds Number Hydrodynamics. Prentice-Hall, Inc., Englewood Cliffs, NJ.

Hebbel, R. P. 1991. Beyond hemoglobin polymerization. The red blood cell membrane and sickle disease pathophysiology. *Blood.* 77:214–237.

Hofrichter, H. J., H. R. Sunshine, F. A. Ferrone, and W. A. Eaton. 1981. Oxygen binding and the gelation of sickle cell hemoglobin. *In* The Molecular Basis of Mutant Hemoglobin Dysfunction. P. B. Sigler, editor. Elsevier North Holland, Inc., New York. 225–236.

Klug, P. P., L. S. Lessin, and P. Radice. 1974. Rheological aspects of sickle cell disease. *Arch. Intern. Med.* 133:577–590.

LaCelle, P. L. 1970. Alteration of membrane deformability in hemolytic anemias. *Semin. Hematol.* 7:355–371.

LaCelle, P. L., E. A. Evans, and R. M. Hochmuth. 1977. Erythrocyte elasticity, fragmentation and lysis. *Blood Cells (NY).* 3:335–350.

Lessin, L. S., J. Kurantsin-Mills, and H. B. Weems. 1977. Deformability of normal and sickle erythrocytes in a pressure-flow filtration system. *Blood Cells (NY).* 3:241–262.

Linderkamp, O., and H. J. Meiselman. 1982. Geometric, osmotic, and membrane mechanical properties of density-separated human red cells. *Blood.* 59:1121–1127.

Messer, M. J., and J. W. Harris. 1970. Filtration characteristics of sickle cells: rates of alteration of filterability after deoxygenation and reoxygenation, and correlations with sickling and unsickling. *J. Lab. Clin. Med.* 76:537–547.

Messmann, R., S. Gannon, S. Sarnaik, and R. M. Johnson. 1990. Mechanical properties of sickle cell membranes. *Blood.* 75:1711–1717.

Mohandas, N., W. M. Phillips, and M. Bessis. 1979. Red blood cell deformability and hemolytic anemias. *Semin. Hematol.* 16:95–114.

Nash, G. B., and H. J. Meiselman. 1982. Red cell and ghost viscoelasticity. *Biophys. J.* 43:63–73.

Nash, G. B., C. S. Johnson, and H. J. Meiselman. 1984. Mechanical properties of oxygenated red blood cells in sickle cell (HBSS) disease. *Blood.* 63:73–82.

Nash, G. B., C. S. Johnson, and H. J. Meiselman. 1986. Influence of oxygen tension on the viscoelastic behavior of red blood cells in sickle cell disease. *Blood.* 67:110–118.

Noguchi, C. T., and A. N. Schechter. 1985. Sickle hemoglobin polymerization in solution and in cells. *Annu. Rev. Biophys. Biophys. Chem.* 14:239–263.

Noguchi, C. T., D. Torchia, and A. N. Schechter. 1980. Determination of deoxyhemoglobin S polymer in sickle erythrocytes upon deoxygenation. *Proc. Natl. Acad. Sci. USA.* 77:5487–5491.

Pfafferott, C., G. B. Nash, and H. J. Mdiselman. 1985. Red blood cell deformation in shear flow. Effects of internal and external phase viscosity and of in vivo aging. *Biophys. J.* 47:695–704.

Reinhart, W. H., S. Usami, E. A. Schmalzer, M. L. Lee, and S. Chien. 1984. Evaluation of red blood cell filterability test: influences of pore size, hematocrit level, and flow rate. *J. Lab. Clin. Med.* 104:501–516.

Rodgers, G. P., A. N. Schechter, C. T. Noguchi, H. G. Klein, A. W. Nienhuis, and R. F. Bonner. 1984. Periodic microcirculatory flow in patients with sickle cell disease. *N. Engl. J. Med.* 311:1534–1538.

Schechter, A. N., C. T. Noguchi, and G. P. Rodgers. 1987. Sickle cell disease. *In* The Molecular Basis of Blood Diseases. G. Stramatoyannopoulos et al., editors. W. B. Saunders Co. pp. 179–218.

Secomb, T. W., R. Skalak, N. Özkaya, and J. F. Gross. 1986. Flow of axisymmetric red blood cells in narrow capillaries. *J. Fluid Mech.* 163:405–423.

Shohet, S. B., and N. Mohandas. 1988. Red Cell Membranes. Churchill-Livingston, Inc., New York.

Skalak, R. 1969. Deformation of red cells in capillaries. *Science (Wash. DC).* 164:717–719.

Sorette, M. P., M. G. Lavenant, and M. R. Clark. 1987. Ektacytometric measurement of sickle cell deformability as a continuous function of oxygen tension. *Blood.* 69:316–323.

Tözeren, H., and R. Skalak. 1978. The steady flow of closely fitting imcompressible elastic spheres in a tube. *J. Fluid Mech.* 87:1–16.

Weed, R. I., P. L. LaCelle, and E. W. Merrill. 1969. Metabolic dependence of red cell deformability. *J. Clin. Invest.* 48:795–809.